Shape Casting: 6th International Symposium
Edited by: Murat Tiryakioğlu, Mark Jolly, and Glenn Byczynski
TMS (The Minerals, Metals & Materials Society), 2016

REAL-TIME RADIOGRAPHY AND MODELING OF POROSITY FORMATION IN AN A356 ALUMINUM ALLOY WEDGE CASTING

Vahid Khalajzadeh[1], David D. Goettsch[2], Christoph Beckermann[1*]

[1]Department of Mechanical and Industrial Engineering, University of Iowa, Iowa City, IA 52242, USA
[2]GM Manufacturing Engineering, Pontiac North CET, Pontiac, MI 48340, USA

Keywords: Real-time Radiography, Shrinkage Porosity, Image Processing, Computational Model

Abstract

The formation of shrinkage porosity in a wedge-shaped A356 aluminum casting is observed in real-time using video radiography. From this observation, an image-processing technique is developed to quantify the through-thickness average porosity distribution in the casting as a function of time. The solidification and cooling of the casting are simulated in order to obtain the temperature and solid-fraction fields. It is found that once the wedge becomes isolated from the in-gate, surface sinks develop until the solid-fraction at the sinking location reaches approximately 45%. Subsequently, internal porosity starts forming in the upper part of the wedge. This interdendritic porosity spreads over the region with the lowest solid-fraction and continually increases until the casting is fully solidified. The maximum porosity percentage is measured in the thermal center of the wedge. A computational model is proposed to predict the evolution of the porosity in the aluminum casting.

Introduction

The complexity of aluminum cast components has steadily increased as the automotive industry strives for mass reduction, higher content and improved fuel economy. Wall stock additions to maintain solidification feed paths add mass back into the design and is the compromise between castability and component weight. Accurate solidification shrinkage porosity models are required to achieve the optimal solution. Solidification shrinkage porosity in aluminum castings are a common industry problem, having a negative impact on the mechanical properties and pressure tightness of cast components [1, 2]. These defects are formed in the mushy zone of the metal as liquid material must compensate for the volume contraction of the solidifying region. If the liquid feed path is insufficient, shrinkage defects of two main categories may form: surface sinks and internal porosities.

Several mathematical and numerical models have been developed to predict the formation of porosity defects in castings. Almost all of the available models originate from the one-dimensional (1-D) model of Piwonka and Flemings [3] and the two-dimensional (2-D) model of Kubo and Pehlke [4]. In review papers by Lee et al. [5] and Stefanescu [6], different porosity models have been discussed. Scientists' advancement of new mathematical models for porosity defects requires precise experimental data for model calibrations. The standard method for quantification of porosity defects is metallographic investigation. But, as this method is not an in-situ approach, it cannot provide extensive information about porosity behavior during

solidification. Therefore, real-time X-ray radiography has become an increasingly popular approach in solidification studies. In a series of experimental studies, Lee et al. [7,8] and Arnberg and Mathiesen [9] have shown that the real-time X-ray is a powerful tool for direct observation of microporosity formation during solidification of aluminum alloys.

In this paper, a real-time video radiography technique is used for observation of shrinkage porosity evolution in a wedge-shaped A356 aluminum casting. In order to process the real-time radiographic video, it is converted to a sequence of images. Next, by developing an image processing algorithm, the radiographic images are processed to obtain the porosity distribution within the casting. In order to predict the transient temperature and solid-fraction fields, the MAGMASOFT® software package is used for thermal simulations. Finally, based on the real-time observations and thermal simulation results, a computational model is developed for the prediction of shrinkage porosity in castings.

Experiments

Internal porosity in aluminum alloys tends to form in the thermal mass center of the casting, the last region to solidify. Two identical wedge castings were considered for experimental investigation to examine the evolution of shrinkage porosity in A356 aluminum alloys. One of the castings was used for temperature measurement and the other used for real-time radiography. Details about the casting geometry and mold dimensions can be found in figure 1.

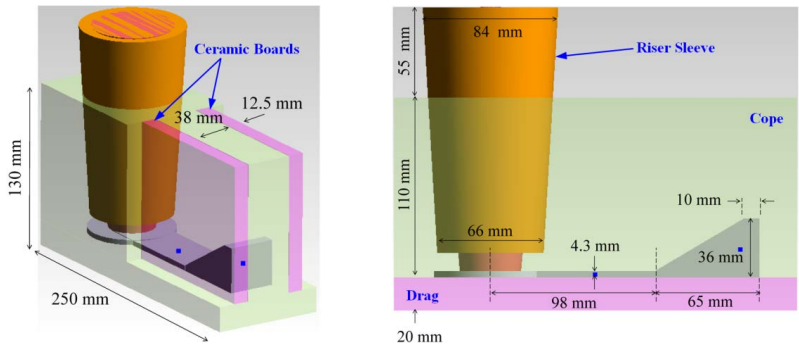

Figure 1. Schematic of castings (a) 3D view, (b) side view

To minimize unwanted artifacts in the radiographic video, two insulating ceramic boards with a thickness of 12.5 mm were used as the front and back mold walls (figure 1(a)). The experimental work was carried out at General Motors Company (GM) where a 450 kV X-ray beam was used for real-time radiography. Photos of the experimental setup and respective facilities can be seen in figure 2. The gas (hydrogen) content in the melt was negligibly small.

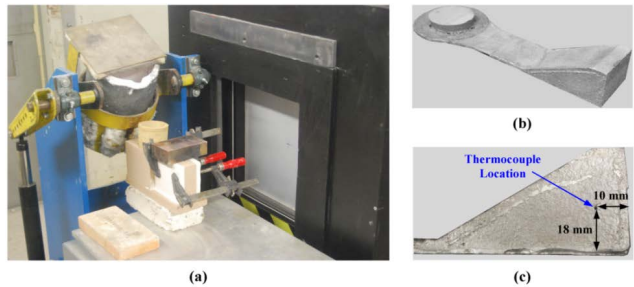

Figure 2. Photos of experimental setup (a) mold and imaging facilities, (b) wedge casting, (c) location of thermocouple on the wedge casting

Porosity Measurement

To process the recorded radiographic video, it is first converted to a sequence of radiographic images. As shown in figure 3(a), in processing of the radiographic images, the brightest and darkest regions on the radiographic images correspond to 100% and 0% porosity areas, respectively. Thus, by assuming that the porosity varies linearly between those two values, the equation for the calculation of pore-fraction is defined as: $g_p(\%) = \left[(v - v_0)/(v_{100} - v_0)\right] \times 100$; where, the v_0 and v_{100} are averaged pixel values of 100% and 0% porosity areas, respectively. As at the vicinity of the casting's surfaces, the pixel values smoothly change to v_{100}, the edges are not clearly distinguishable on the images. Therefore, for tracking the surface movement and separating the internal porosity from the surface sink, a surface mask is used. Once the pore-fraction field is defined, one can calculate the total shrinkage by taking an average over the entire field. As shown in figure 3(b), after the runner freezes off at 8 s, a sink starts to develop on the inclined surface. This sink continues to grow until about 90 s. Then, internal porosity forms in the thermal center of the wedge, and it grows until the casting is fully solidified. In figure 3(b), the total shrinkage is the sum of the surface sink and internal porosity fractions.

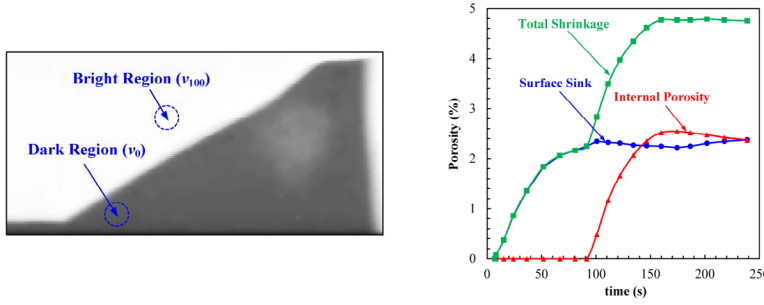

Figure 3. (a) Bright and dark regions on a sample image, (b) variation of measured surface sink, internal porosity and total shrinkage with time

Thermal Simulation

In order to calculate the thermo-physical properties of the A356 aluminum alloy, the composition in table 1 was entered into the JMatPro software package [10]. Then, by applying the exact experimental conditions, the casting was simulated using the MAGMASOFT® software package. The solidus and liquidus temperatures and the solid fraction vs. temperature curve were adjusted using cooling curve analysis. The temperature dependent interfacial heat transfer coefficient between the casting and the mold was obtained using a trial-and-error procedure. Figure 4 shows that after all adjustments were made, the measured and predicted temperatures at the location of thermocouple are in excellent agreement.

Table 1. A356 aluminum alloy composition, given in weight percent

	Cu	Fe	Mg	Mn	Ni	Si	Sr	Ti	Zn
A356 aluminum	0.001	0.09	0.38	0.006	0.004	7.05	0.001	0.11	0.002

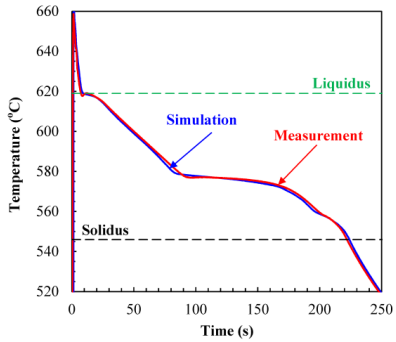

Figure 4. Measured and simulated temperature results at the location of thermocouple

Porosity Modeling

A new porosity formation model was developed to predict the evolution of the surface sink and internal shrinkage in the wedge casting. First, using the predicted temperature fields from MAGMASOFT®, density fields are obtained using the density vs. temperature curve shown in figure 5(a). Then, the total solidification shrinkage (β) for the wedge and the total shrink volume (ΔV_{Shrink}) at each time step, are calculated using equations (1) and (2):

$$\beta(t_n) = \frac{V(t_0) - V(t_n)}{V(t_0)} = 1 - \left(\frac{\sum_{i=1}^{N_{nodes}} \rho_i(t_0)}{\sum_{i=1}^{N_{nodes}} \rho_i(t_n)} \right) \quad (1)$$

$$\Delta V_{Shrink}(t_n) = V(t_{n-1}) - V(t_n) = \left(\beta(t_n) - \beta(t_{n-1}) \right) \times V(t_0) \quad (2)$$

where, $V(t_n)$ denotes the total volume at time t_n, $\rho_i(t_n)$ is the alloy density at cell *i* and time t_n, and N_{node} is total number of computational cells. As seen in figure 5(b), there is reasonably good agreement between the measured and predicted evolutions of the total shrinkage porosity in the wedge. Any discrepancies can be attributed to the approximate nature of the method used to obtain the porosity values from the radiographic images.

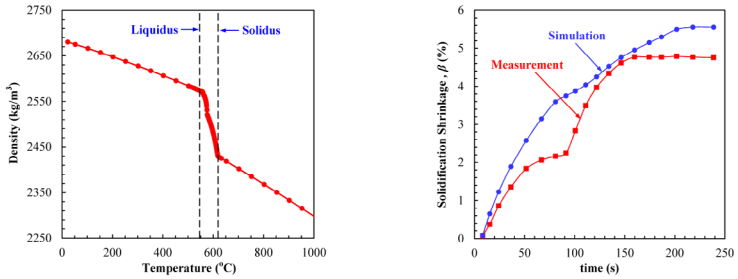

(a) **(b)**

Figure 5. (a) A356 aluminum alloy density variation with temperature, (b) Comparison of measured and predicted total shrinkage values

Based on the present real-time radiographic observations, the evolution of the shrinkage porosity in the wedge casting consists of two stages. In the first stage, after the wedge becomes isolated from the in-gate, surface sinks form. A surface is assumed to be able to sink until the local solid fraction reaches a certain coherency value, i.e., $g_s < g_{s,coh}$. Internal porosity can form only in a second stage, after the entire surface of the wedge has reached the coherency limit. The total shrinkage volume, ΔV_{Shrink}, at each time step is allocated only to surface cells during the first step and only to internal cells during the second stage.

In order to decide which computational cells can receive the shrinkage volume ΔV_{Shrink}, a new parameter, Π, is defined as:

$$\Pi = \left(1 - g_s\right)\left(\frac{P_{max} - P}{P_{max}}\right)^{\alpha} \tag{3}$$

where, g_s is the solid fraction, P is the hydrostatic pressure, P_{max} is the maximum hydrostatic pressure, and α is an adjustable exponent. The shrinkage volume is distributed to cells that are within a certain range of Π values, i.e., $\Pi_{Active} < \Pi < \Pi_{Max}$, where, Π_{Max} is the maximum value of Π and Π_{Active} is another adjustable parameter. A typical value for Π_{Active} is $0.95\,\Pi_{Max}$. The total volume of the active cells, ΔV_{Active}, should always be greater than ΔV_{Shrink}; if not, Π_{Active} is reduced until $\Delta V_{Active} = \Delta V_{Shrink}$. Cells that have a Π value within the range $\Pi_{Active} < \Pi < \Pi_{Max}$ are called active cells. Examples of active cell distributions are shown in figure 6. The present

definition of the Π parameter assumes that porosity forms only in cells with the lowest solid fractions. The second factor in equation (3) accounts for the fact that the hydrostatic pressure plays a role too. For example, if the solid fraction is the same everywhere (e.g., pure liquid), only the cells with the lowest hydrostatic pressure are active. The exponent α allows one to weigh the importance of the pressure effect. The total shrinkage volume is distributed evenly across all active cells. Hence, the change in the porosity volume fraction of each active cell can be calculated from $\Delta g_p = \Delta V_{Shrink} / \Delta V_{Active}$.

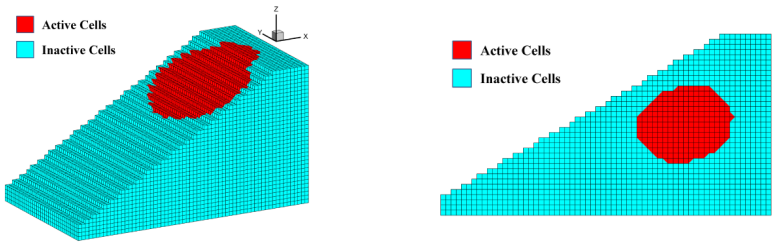

(a) **(b)**

Figure 6. Typical examples of active cell distributions: (a) surface sink, (b) internal porosity

Results

Figure 7 shows a comparison of measured and predicted porosity distributions at three different times. The original radiographic images and the computed solid fraction distributions are also provided in the figure. At the time the surface stops sinking (around 90 s), the minimum solid fraction on the surface of the wedge is about 45% [see figure 7(h)]. Hence, the coherency solid fraction, $g_{s,coh}$, is chosen as 0.45. Interestingly, this solid fraction corresponds approximately to the start of the eutectic formation in the A356 alloy. Numerous simulations were performed where α and Π_{Active} were varied until the measured and predicted porosity distributions agreed best. The optimum combination of these adjustable parameters was found to be $\Pi_{Active} = 0.965\Pi_{Max}$ and $\alpha = 0.14$. With this combination of parameters both the sink on the inclined surface and the internal porosity near the thermal center of the wedge are predicted well.

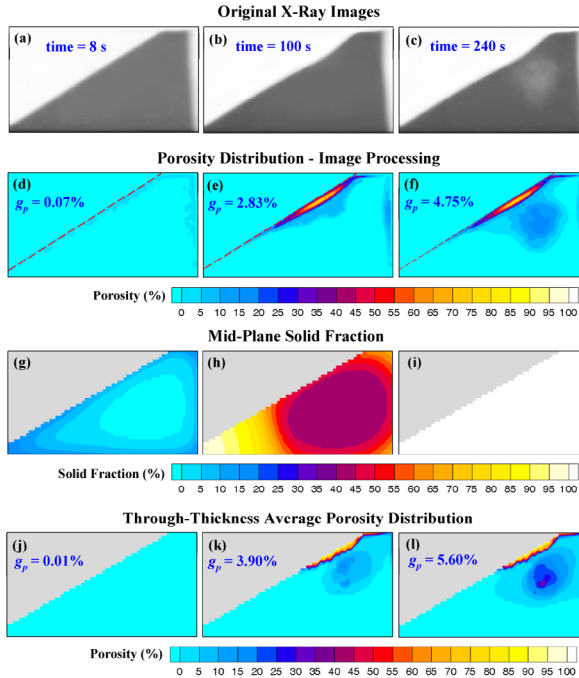

Figure 7. Comparison of measured and predicted results at 8s (left column), 100 s (middle column), and 240 s (right column): (a)-(c) original radiographic images, (d)-(f) processed radiographic images showing the measured porosity distribution, (g)-(i) predicted mid-plane solid fraction distributions, (j)-(l) predicted through-thickness average porosity; the model uses $\Pi_{Active} = 0.965\Pi_{Max}$ and $\alpha = 0.14$.

Conclusion

Formation of shrinkage porosity in an A356 aluminum alloy wedge casting is observed using a real-time video radiographic technique. By developing an image processing procedure, the recorded video is processed to obtain the porosity distribution in the casting as a function of time during solidification. It is shown that the porosity evolution in the wedge consists of two stages: 1) surface sink formation and 2) internal porosity formation. The surface sink starts when the wedge becomes isolated from the feeder and continues until the surface becomes coherent. Then, internal porosity forms in the area with lowest solid fraction. Based on the experimental observations, a model is developed to predict the shrinkage porosity formation in the wedge. Comparison between the simulation and experimental results shows that the proposed method can reasonably predict the location and distribution of shrinkage porosity.

Acknowledgements

The authors wish to thank Anil Sachdev, Gene Tuohy, Mike Walker and Jason Traub for their support of the foundry real-time x-ray room at GM R&D and the work on this project.

References

[1] M. J. Couper, A. E. Neeson, and J. R. Griffiths, "Casting defects and the fatigue behaviour of an aluminium casting alloy," *Fatigue & Fracture of Engineering Materials & Structures*, 13 (1990), 213-227.

[2] Q. G., Wang, D. Apelian, and D. A. Lados, "Fatigue behavior of A356-T6 aluminum cast alloys, Part I. Effect of casting defects," *Journal of Light Metals* , 1 (2001), 73-84.

[3] T. S. Piwonka and M. C. Flemings, "Pore formation in solidification," *AIME MET SOC TRANS* , 236 (1966), 1157-1165.

[4] K. Kubo and R. D. Pehlke, "Mathematical modeling of porosity formation in solidification," *Metallurgical Transactions B* , 16 (1985), 359-366.

[5] P. D. Lee, A. Chirazi, and D. See, "Modeling microporosity in aluminum–silicon alloys: a review," *Journal of Light Metals*, 1 (2001), 15-30.

[6] D. M. Stefanescu, "Computer simulation of shrinkage related defects in metal castings–a review," *International Journal of Cast Metals Research*, 18 (2005), 129-143.

[7] P. D. Lee and J. D. Hunt, "Hydrogen porosity in directional solidified aluminium-copper alloys: in situ observation," *Acta Materialia* , 45 (1997), 4155-4169.

[8] R. C. Atwood, S. Sridhar, W. Zhang, and P. D. Lee, "Diffusion-controlled growth of hydrogen pores in aluminium–silicon castings: in situ observation and modelling," *Acta materialia*, 48 (2000), 405-417.

[9] L. Arnberg and R. H. Mathiesen , "The real-time high resolution x-ray video microscopy of solidification in aluminum alloys," *JOM*, 59 (2007), 20-26.

[10] JMatPro, Sente Software Ltd, Surrey Technology Center, Surrey GU2 7YG, United Kingdom.